

NASA TECHNICAL NOTE



NASA TN D-4156

e.1

LOAN COPY
APR 1967
KIRTLAND



NASA TN D-4156

THEORETICAL PERFORMANCE OF SOLAR-CELL SPACE POWER SYSTEMS USING SPECTRAL DISPERSION

I - Dispersion by Prism Reflector

by Anthony F. Ratajczak

Lewis Research Center

Cleveland, Ohio



THEORETICAL PERFORMANCE OF SOLAR-CELL SPACE
POWER SYSTEMS USING SPECTRAL DISPERSION
I - DISPERSION BY PRISM REFLECTOR

By Anthony F. Ratajczak

Lewis Research Center
Cleveland, Ohio

NATIONAL AERONAUTICS AND SPACE ADMINISTRATION

For sale by the Clearinghouse for Federal Scientific and Technical Information
Springfield, Virginia 22151 - CFSTI price \$3.00

THEORETICAL PERFORMANCE OF SOLAR CELL SPACE POWER SYSTEMS USING SPECTRAL DISPERSION

I - DISPERSION BY PRISM REFLECTOR

by Anthony F. Ratajczak

Lewis Research Center

SUMMARY

The concept of using dispersed solar energy to power solar cells that have spectral responses matched to particular portions of the solar spectrum was analyzed. The analysis was divided into several parts: the prism reflector, the refraction losses and the effect of the sun's cone of light on the dispersed beam, and an estimate of the overall system energy-conversion efficiency using hypothetical solar cells.

The analysis revealed that maximum dispersion (i. e. , maximum angular separation between the refracted blue and red rays) is attended by a large loss in optical system efficiency. Maximum dispersion, however, is necessary to counter the manner in which the cone of light from the sun spoils the monochromaticity of the spectral beam. The approximate overall optical efficiency of a collector and a prism-reflector element, which produces near maximum dispersion, is 56 percent.

Regardless of the efficiency of the optical system, it was of interest to evaluate the conversion efficiency of the solar-cell array. In spite of optimistic assumptions regarding both the quality of the spectral light reaching the cells and the efficiencies of the various cells, the array conversion efficiency was calculated to be only 14 percent. Thus, the combined efficiency of the optical system (56 percent) and the solar-cell array (14 percent) yields an overall system efficiency of only about 8 percent. Such a concept, therefore, offers no improvement over present day white-light solar-cell arrays, which are about 9 percent efficient in space.

INTRODUCTION

Conventional solar-cell space power systems expose the solar cells to most of the

solar spectrum. Approximately 27 percent of the solar energy is reflected or converted directly into heat in the cell. Of the remaining 73 percent, only about 13 percent is converted into electricity. Thus, the nominal 10-percent-efficient conventional silicon solar cell makes relatively inefficient use of solar energy.

To make better use of the sun's energy, a system was proposed that would focus a spectrum of light on several different types of solar cells, each type having a different spectral response range (fig. 1). The optical system required to produce this spectral light would consist of a parabolic collector to focus the sun's energy on a prism reflector or a diffraction grating. (This report analyzes the prism reflector, and a companion report, Part II by Thomas M. Klucher (ref. 1), the diffraction grating.) Each type of solar cell would then be placed in that portion of the dispersed beam appropriate to its spectral response.

The proposed system might be more efficient because, for each wavelength of the useable portion of the solar spectrum (nominally from 0.36 to 1.2 μm), the solar cells could be selected for maximum efficiency at that wavelength. Also, since the cells would not receive unuseable radiation, they should operate cooler and, therefore, more efficiently.

On the other hand, the system has several built-in inefficiencies which must be more than offset by increased cell performance to make the concept worthwhile. There are, for example, light energy losses at the reflecting and refracting surfaces and during transmission in the prism. In addition, since the sun is not a point source of light and its rays are therefore not parallel, it is not possible to achieve perfect monochromaticity in the dispersed spectral beam.

This analysis, therefore, separately examined, first, the inefficiencies of the proposed optical system, and then, the potential advantage of a multiple-type cell array, including only the factor of nonparallel light. The separate results are then combined to show the overall potential of such a system.

PRISM-REFLECTOR FUNDAMENTALS

There are three fundamental parameters that determine prism-reflector design. These are (from fig. 2) the incidence angle of the white light θ_1 , the total dispersion, or simply the difference between the emergence angles of the blue and red spectral extremes $\Delta\theta_4$ (0.36 and 1.2 μm , respectively), and the prism wedge angle β .

The angle at which any wavelength ray leaves the prism reflector $\theta_{4,\lambda}$ can be found as follows. Referring to figure 2(b) and applying Snell's law yields

$$\frac{\sin \theta_{12, \lambda}}{N} = \frac{\sin \theta_1}{n_\lambda} \quad (1)$$

where

N spectral refractive index of vacuum, assumed to be 1

n_λ spectral refractive index

$$\theta_{2, \lambda} = \theta_{12, \lambda} + \beta \quad (2)$$

$$\theta_{3, \lambda} = \theta_{2, \lambda} + \beta \quad (3)$$

and

$$\sin \theta_{4, \lambda} = n_\lambda \sin \theta_{3, \lambda} \quad (4)$$

A more convenient expression for $\theta_{4, \lambda}$, derived by substituting equation (3) into equation (4) and expanding, is

$$\sin \theta_{4, \lambda} = \sin 2\beta \sqrt{n_\lambda^2 - \sin^2 \theta_1} + \sin \theta_1 \cos 2\beta \quad (5)$$

Equation (5) relates incidence angle, prism-reflector wedge angle, wavelength, and emergent angle and is used to calculate dispersion by

$$\Delta\theta_4 = \theta_{4, B} - \theta_{4, R} \quad (6)$$

The spectral index of refraction n_λ for any glass may be calculated for any wavelength (ref. 2) by

$$n_\lambda = A + \frac{B}{2} + \frac{C}{4} + \dots \quad (7)$$

where A , B , and C are constants dependent on the material and are, for heavy flint glass, which was chosen for the prism-reflector material (ref. 3), 1.6144, 0.01083, and -0.001083, respectively. Three terms give sufficient accuracy for most calculations.

These equations provide the basis for examining prism-reflector characteristics. Figure 3 shows the relation of the fundamental prism-reflector parameters and also defines some practical limits in terms of the system concepts defined in figure 1. First, since shorter wavelengths are refracted most, the incidence angle of the white light is limited by the emergent angle of the extreme blue ray $\theta_{4,B}$ since $\theta_{4,B}$ cannot exceed 90° . Secondly, as shown in the system configurations (fig. 1) and the prism-reflector description (fig. 2(a)), the incidence angle θ_1 cannot fall in the region between $\theta_{4,B}$ and $\theta_{4,R}$. Were θ_1 in that region, the incident energy would come from the position to be occupied by the solar-cell array. Thus, for any value of prism wedge angle β , there is a certain range of values of the incidence angle θ_1 that is prohibited. It follows that there is also, for any value of prism wedge angle, a range of dispersion values that are unobtainable. For prism-reflector parameters producing values of maximum dispersion, the incident beam falls in the region between $\theta_{4,B}$ and $\theta_{4,R}$ (fig. 3) and thereby precludes those dispersion values. It remains to be shown that maximum dispersion is a necessary factor.

At this point in the discussion, therefore, two factors limit prism-reflector design: the angle of the emerging blue ray, which obviously cannot exceed 90° , and the position of the incident ray relative to the emerging dispersed beam. The energy losses at the re-refracting surface must also be considered, however, and these are discussed in the next section.

ENERGY LOSS IN PRISM REFLECTOR

When light passes through a refractive interface, some of the light is refracted and some reflected, according to the angle of the incident ray. The fraction of the incident light reflected parallel and perpendicular to the plane of incidence, r_p and r_s , respectively, is given by (ref. 4)

$$r_p = \frac{[-\sin(\varphi_1 - \varphi_2)]^2}{[\sin(\varphi_1 + \varphi_2)]^2} \quad (8)$$

$$r_s = \frac{\tan^2(\varphi_1 - \varphi_2)}{\tan^2(\varphi_1 + \varphi_2)} \quad (9)$$

where

φ_1 absolute value of incidence angle

$\varphi_2 \sin^{-1}(\sin \varphi_1/n_\lambda)$

The percent of the total incident energy that is refracted at each surface is given by

$$E_r = \frac{2 - (r_p + r_s)}{2} \times 100 \quad (10)$$

Figure 4 shows the percentage of the incident intensity of blue and red light that is refracted at the prism-reflector surfaces. In this figure there is no correlation between the incidence angles of the first and third prism-reflector surfaces or between the blue and red incidence angles at a surface.

As shown in figure 4, the refraction losses for blue light at the prism third surface, glass to air, set a limit of 36° on the blue-light incidence angle at that surface $\theta_{3,B}$.

Refraction losses at the prism-reflector third surface and the system configuration restraint of noncoincidence between incident white light and the dispersed beam combine to impose limitations on dispersion and total refracted light. A brief sample calculation will aid in understanding the situation.

Assume that an 11.5-percent loss of blue light at the third surface is tolerable (fig. 4). This loss corresponds to a $\theta_{3,B}$ of 30° . Now, from figure 5 which shows the relation of $\theta_{3,B}$ to prism-reflector parameters, assume the prism wedge angle β is 25° and then dispersion $\Delta\theta_4$ is 6.4° . For a dispersion of 6.4° and a prism wedge angle of 25° , $\theta_{4,B}$ is 60° , and $\theta_{4,R}(\theta_{4,B} - \Delta\theta_4)$ is 53.6° (fig. 3). Thus, there is no coincidence between the incident and the emerging beams since $\theta_{4,R}$ (53.6°) is greater than the absolute value of θ_1 (35°).

Given the requirement for maximum dispersion, the 6.4° achieved for this case compares unfavorably with a potential maximum of 24° . To increase dispersion without increasing refraction losses at the third surface requires a larger prism wedge angle β and, correspondingly, a greater first-surface incidence angle θ_1 . However, as the wedge angle, the absolute value of the incidence angle, and the dispersion increase (fig. 6(a)), the incident ray eventually intercepts the emerging red ray. From the value of wedge angle at that point until the wedge angle has increased to where the incidence angle θ_1 is greater than the angle of the emerging blue ray, the incident ray and the emerging beam are coincident. Therefore, values of dispersion from about 7.3° to 7.7° (fig. 6(b)) are precluded by the system configuration restraint of noncoincidence. To achieve values of dispersion greater than 7.7° requires an incidence angle of about 69° or higher. At this incidence angle (fig. 4), the blue-light refraction loss at the first surface is 20 percent or greater. Therefore, refraction losses at the first and the third surfaces of the prism reflector and the system requirement of noncoincidence restrict dispersion to a

narrow range of relatively low values.

Another energy loss in the prism reflector is the reflection loss at the reflecting surface. Reflection from a silvered surface (ref. 5) is almost a constant 90 percent for a wide range of incidence angles (0° to 70°). The range of incidence angles at the second (silvered) surface of the prism reflector θ_2 is sufficiently low ($< 30^{\circ}$) to conclude that there will be essentially 90-percent reflection from that surface.

One further consideration is the reflection loss at the primary collector. Again, for a silvered surface and within the range of practical rim angles (to 60°), the loss will be about 10 percent.

SOLAR-CONE-ANGLE EFFECT

The sun is not a point source of light but subtends an angle of $32'$ from earth. The fact that the light rays are not parallel has an effect on the performance of the optical system since every point on the solar collector receives and, therefore, reflects a cone of light. Instead of the actual circular or three-dimensional situation, a simplified or two-dimensional case (viz, a plane of radiation parallel to and through the optic axis of the collector) was considered to simplify the analysis of the effect of the cone of light on dispersion. The normal ray (fig. 7) is defined as that ray which comes from the center of the solar disk. The positive and negative cone rays come from the edge of the disk. ("Cone" ray is now understood to mean a ray coming from the edge of the wedge or "cone" of light.) In figure 7, φ' is the angle between normal ray (1) and the optic axis at the focus; f is the focal length; x , some fraction of the focal length, is the distance from the focus to the plane of the prism reflector; y is the distance from the optic axis to the point on the prism-reflector plane where a cone ray intersects with either normal ray (2) or (3); and δ , the angle between the positive or negative cone rays and the normal rays (2) or (3) at the prism-reflector surface, is defined as the deviation. In the remainder of this analysis, δ and y are understood to refer to the positive cone ray unless otherwise indicated.

Figure 7 shows generally what happens to the deviation angle δ as the prism-reflector plane is moved along the optic axis. As the plane moves close to the solar collector (and at the same time becomes larger in diameter), the absolute value of the deviation angle δ decreases since normal ray (2) approaches normal ray (1). In the other extreme, the prism-reflector plane approaches the focus and results in increasing deviation since normal ray (2) approaches the optic axis. The expressions for the deviation angle δ for either half of the cone of light as a function of φ' as determined by normal ray (1) and the position of the prism reflector on the optic axis are

$$\delta_+ = \varphi' + \alpha - \tan^{-1} \frac{y}{x} \quad (12a)$$

$$\delta_- = -\varphi - \alpha + \tan^{-1} \frac{y}{x} \quad (12b)$$

where x is the focal length fraction,

$$y = \left[x - \frac{2f (\sin \alpha \sin \varphi')}{(1 + \cos \varphi') \sin (\varphi' + \alpha)} \right] \tan (\varphi' + \alpha)$$

α is plus or minus 16' of arc, δ is positive or negative corresponding to a positive or negative α , and φ' is the angle between normal ray (1) and the optic axis at the focus. Thus, either the focal length must be very long (low rim angle) or the plane of the prism reflector must be close to the collector to minimize the deviation angle, which is shown later to be a most desirable case.

Figure 8 shows the deviation angle δ of the positive cone of light for various positions of the prism-reflector plane on the collector optic axis. Only the positive cone-ray variation is shown because for values of x greater than 0.15, the deviations for the positive and the negative cone rays differ by less than 2 percent. A low value of x is desirable to minimize mirror diameter. This minimization in turn, however, increases the cone-ray deviation which, as is shown later, spoils spectral quality. Spectral quality is defined as the degree of monochromaticity of all the light falling on any point of the solar array.

A good understanding of spectral quality and how a prism reflector refracts a cone of white light and, therefore, affects spectral quality is necessary. Figure 7 shows, in general, how, because of the partial cone of light, the blue and red rays are projected on the solar-cell array, that is, a line on the array, instead of only a point, is illuminated by blue or red light (in all cases, blue is 0.36 μm and red is 1.2 μm). Ideally (i. e., if the sun were a point source) only the blue and the red from the normal rays would be present and would illuminate only a point. Between the blue and the red rays shown in figure 7 are, of course, all the wavelengths between 0.36 and 1.2 microns.

An analysis of spectral quality and the cone effect is best accomplished in two steps: first, by describing in detail how the characteristics of a prism-reflector element affect the refraction of the blue and the red extremes, and then by showing a dispersed beam from a prism-reflector element that includes all wavelengths between the extremes. For both cases, it is convenient to assume that there are no losses in the prism reflector and that the deviation angle δ is symmetrical around the normal ray.

For values of prism wedge angle β for which the incident beam was outside the emerging beam, the extreme blue ray was assumed to emerge at $\theta_{4,B} = 90^\circ$ to ensure that the complete cone of light is refracted out of the prism reflector. This assumption allows maximum dispersion. It was further assumed that the blue light for the positive cone ray for any deviation angle δ would emerge at $\theta_{4,B} = 90^\circ$ and that, therefore, the incidence angle θ_1 for this condition represented the incidence angle of the positive cone ray of light. The incidence angle of the normal ray is then $\theta_1 - \delta$, and the incidence angle for the negative cone of light ray, if all rays are assumed to strike the surface at the same point, is $\theta_1 - 2\delta$. Thus, since $\theta_{4,B}$ for the blue positive cone ray is always 90° , θ_1 for the positive cone ray for any wavelength will be a constant for a given prism wedge angle and deviation angle, and $\theta_{4,R}$ will be constant for the red positive cone ray.

Based on the foregoing assumptions, figure 9 shows two effects of refracting the blue and red rays from a cone of white light: first, how, as a function of deviation angle δ , a given wavelength from a cone of light defocuses at the prism reflector third surfaces, and, second, how the wedge angle β of the prism reflector affects the separation between the inside extremes of the refracted red and blue beams.

From figure 9, two conclusions can be drawn regarding prism-reflector and complete optical system design. First, minimum deviation is necessary to minimize defocusing of a given wavelength at the solar-cell array. However, from figure 8, to meet the requirement of minimum deviation requires a relatively high value of x . (Note that fig. 8 does not consider the shadowing of the collector by the prism reflector.) This requirement, in turn, increases collector area (assuming the hole in the center of the collector can be used only for solar cells). Secondly, maximum prism-reflector wedge angle is necessary to increase the separation between the refracted red- and blue-beam inside extremes. Maximum separation is necessary to prevent overlapping of different wavelengths at the solar-cell array.

Having examined the particular case of the refraction of blue and red rays as a function of deviation and prism-reflector wedge angles, the general case, showing all wavelengths is now considered. However, rather than show all wavelengths dispersed as functions of the several variables δ , β , x , and $\Delta\theta_4$, again, a special case was chosen that yielded an optimistic picture of dispersion and spectral quality. Therefore, to the assumptions of the foregoing analysis regarding prism-reflector losses and deviation is added the principal requirement that the prism wedge angle β yield near maximum dispersion without coincidence between the incident and the emerging prism-reflector beams. A prism wedge angle value of 30° satisfies this requirement. Based on these assumptions and this requirement, the manner whereby a prism reflector disperses a cone of white light is shown in figure 10.

Recalling the manner in which the positive cone ray is always placed at θ_1 will aid

in understanding the relation between the positive cone-ray curve and the other curves labeled according to the different values of deviation for which they represent the negative cone spectral extreme. The ordinate in figure 10 is in degrees of θ_4 . The area of the array, represented by an angle $(\Delta\theta_4)_{a,b}$ illuminated by a particular wavelength is read between the positive cone curve and whatever deviation curve is used. If the ordinate is taken to represent the solar-cell array, which in principle it does, then the distance between the positive cone ray and any deviation represents directly the spectral quality and intensity at any point on the solar-cell array. Spectral quality may be read from any point on the ordinate along a line parallel to the abscissa. The region bounded on the left by the value of deviation selected (δ , 16' to 80') and on the right by the positive cone curve is, in terms of the wavelength values so bounded, the spectral quality at that point on the array (for values of θ_4 lower than 68° , the solar-cell response cutoff is 1.18 μm). In this respect, the greater the difference between the wavelength values, the poorer the quality.

The spectral intensity can also be determined from figure 10. The actual solar spectral intensity in a wavelength interval $\Delta\lambda$ is contained within an area bounded by the positive cone curve and the deviation curve. Therefore, the spectral intensity ($\text{mW}/(\text{cm}^2)(\Delta\lambda)$) illuminating an area $(\Delta\theta_4)_{a,b}$ of the solar array is proportional to the ratio of the area of $\Delta\lambda$ within the limits of $\Delta\theta_4$ to the whole area of $\Delta\lambda$ between the deviation curves. Thus, figure 10 forms a complete picture of the solar-cell array as illuminated by a prism-reflector element.

The monochromaticity, or spectral quality, is easily seen to be a function of deviation and prism-reflector wedge angle. Increasing the wedge angle substantially improves spectral quality for all values of deviation.

The curve of average third-surface refraction efficiency (for $\delta = 64'$) was added to figure 10 to make the refraction picture more complete. It shows that the highest quality portion of the dispersed beam suffers the most from third-surface refraction losses which, added to the fact that that portion of the beam is also spread out over almost 50 percent of the array area, permits a substantial portion of the array to produce only a very small percentage of the total array power. Included in this unfortunate combination of inefficiency factors is the additional fact that about 16 percent of the sun's intensity is between 0.36 and 0.5 microns. Therefore, the loss imposed on overall conversion efficiency becomes quite high. It is interesting, nevertheless, to pursue the analysis one step further and to obtain some value of energy-conversion efficiency (light to electricity).

SOLAR-CELL AND ARRAY CONVERSION EFFICIENCY

The proposed system concept called for the placing of solar cells with different

response ranges (i. e. , with peak response at different wavelengths) in appropriate portions of the spectral beam. A review of the spectral response characteristics of all available solar cells, in various stages of development, showed that the wavelength range of spectral response of all cell types was from about 0.3 to 1.2 microns, which is approximately the total response range of silicon.

Since the prism-reflector analysis already had cast some doubt on any potential solar-cell system improvement, and since the types of solar cells required are well beyond the state-of-the-art, a simplifying assumption was in order. Accordingly, it was assumed that the spectral response curve for the n-p silicon solar cell (fig. 11) could be transposed along the wavelength scale and could thereby have its maximum response point centered on any wavelength between 0.36 and 1.18 microns.

Such an assumption allows a great deal of latitude in selecting the position on the array for a particular cell. Therefore, it was further assumed that to take maximum advantage of the quality of the dispersed spectral beam for $\beta = 30^\circ$ and $\delta = 64'$ (fig. 10) there should be a different cell (meaning a different maximum response wavelength) for every 1° of arc of the dispersed beam. Although dispersion for $\beta = 30^\circ$ and $\theta_{4,B} = 90^\circ$ is 22° (fig. 3), the cone effect causes red light to which a silicon cell responds to extend the array width another 3.5° to 64.5° . The solar-cell array, in order to take maximum advantage of the available light, was therefore considered to extend to 64.5° . This procedure gives an effective dispersion of 25.5° .

Assume now, that a solar-cell array composed of a variety of different cells is illuminated by the $64'$ deviation spectral beam represented in figure 10. Neglecting any losses in the optical system, the following discussion describes the calculation of individual cell efficiencies, weighted solar intensity, and total array conversion efficiency.

The assumptions used to calculate array conversion efficiency are

- (1) There is a different type of cell (spectral cell) in every 1° of arc of the dispersed beam.
- (2) Each of these different cells would have a spectral response wave exactly the same as for the conventional silicon cell except that the maximum-response point of each different cell would roughly correspond to the center wavelength of each 1° interval of the dispersed beam.
- (3) The efficiency calculated for the standard silicon cell for the wavelength interval $\Delta\lambda'_{1,2}$ (fig. 12) would be the efficiency of the cell in the spectral band $\Delta\lambda_{a,b}$ defined by $\theta_{4,a}$ to $\theta_{4,b}$.
- (4) Operating temperature for all cells was assumed to be 28° C.

If it is assumed that the silicon-cell spectral response shown in figure 11 is for a 10 percent cell, the efficiency of each of the spectral cells is given by

$$\eta_i = \frac{K \int_{\lambda_1}^{\lambda_2} R(\lambda) H(\lambda) d\lambda}{\int_{\lambda_1}^{\lambda_2} H(\lambda) d\lambda}$$

where

$$K = \frac{\eta_{si} \int_0^{\infty} H(\lambda) d\lambda}{\int_0^{\infty} R(\lambda) H(\lambda) d\lambda}$$

η_i efficiency of standard 10-percent silicon solar cell when illuminated by light of range $\Delta\lambda'_{1,2}$

η_{si} efficiency of typical 10-percent silicon cell

$R(\lambda)$ standard silicon-cell equal energy relative short-circuit-current spectral response (fig. 11)

$H(\lambda)$ solar spectral intensity

λ_1, λ_2 equal response points wavelengths (from fig. 11)

The specific wavelengths are obtained in the following manner. From figures 10 and 12, the wavelength range $\Delta\lambda'_{1,2} = \lambda'_2 - \lambda'_1$ for any 1° of spectral band ($\theta_{4,a}$ to $\theta_{4,b}$) was taken at the $1/2^0$ point (e.g., for the spectral band $\theta_{4,a} = 71^\circ$ to $\theta_{4,b} = 70^\circ$, $\Delta\lambda'_{1,2}$ was determined between the positive-cone and 64' curves at $\theta_4 = 70.5^\circ$). This value of $\Delta\lambda'_{1,2}$ (0.192 μm) was then used to determine the cell response ($R = 0.89$) at equal response points λ_1 and λ_2 on figure 11.

The output power per unit area from each group of spectral cells P_i is then given by

$$P_i = \sum_{j=\lambda_a}^{\lambda_b} \left(\frac{B_{ij}}{B_j} H_{\lambda_j} \right) \eta_i$$

where

B_{ij}/B_j ratio of area representing solar spectral intensity in the band $\theta_{4,a}$ to $\theta_{4,b}$ and in wavelength interval $\Delta\lambda_{Hj} = 0.02$ microns to area representing total solar spectral intensity in wavelength interval $\Delta\lambda_{Hj}$

H_{λ_j} total solar intensity in wavelength interval $\Delta\lambda_{Hj} = 0.02 \mu\text{m}$

Thus, the total array energy conversion efficiency is

$$\eta = \frac{\sum_{i=1}^{26} P_i}{140}$$

This calculation assumes that there are no losses in the optical system and that the solar concentration ratio is 1.

When these equations are used, the array conversion efficiency for this idealized case is 14.5 percent as compared with 10 percent for a conventional silicon-cell array using the same temperature and input-intensity assumptions.

Because of the cone of light and the refractive properties of a prism, only 4.4 percent of the electric power comes from that portion of the array receiving the highest quality light (arbitrarily, 90° to 78°), whereas 32.2 percent of the power comes from the array area between 68° and 64.5° (poorest quality light).

SUMMARY OF RESULTS

The calculated potential increase in solar-cell-array conversion efficiency must now be considered together with other system factors affecting overall system conversion efficiency. First, although it is doubtful that cells of the assumed efficiencies are in the offing, one of the advantages of the proposed system is that the various cells would operate at lower than normal temperatures and thereby minimize the efficiency loss encountered in conventional arrays. Thus, the assumed cell operating temperature of 28° C should, on the average, be reasonably correct. The silicon cell is 10 percent efficient at 28° C (*laboratory test conditions*) and about 9 percent efficient at operating conditions in space.

Second, there is the broad category of optical system losses. The most critical of these losses is the refraction loss at the prism third surface. From figure 10, average third-surface refraction efficiencies for the prism used in the array conversion-efficiency calculation range from 84 percent at 1.2 microns to 2.6 percent at 0.36 microns. The average third-surface refraction efficiency is therefore about 80 percent. Other factors are the refraction efficiency of the prism first surface, about 95 percent, the reflection efficiency of the prism second surface and of the primary collector, about 90 percent each, and the transmission efficiency of the prism which ranges from 16 percent at 0.36 microns to 90 percent or more at 0.425 to 1.2 microns. Combining all these optical system efficiencies yields an overall optical system efficiency of approximately 55.5 percent, which in turn reduces the overall system conversion efficiency from an ideal 14.5 percent to approximately 8 percent.

CONCLUSIONS

Under ideal conditions, the proposed dispersion concept offers some potential improvement in solar-cell-array conversion efficiency. Real conditions, however, restrict this potential. There is a substantial energy loss in the optical system, and the cone of light from the sun reduces the monochromaticity of the dispersed beam, which in turn detracts from the effectiveness of using dispersed light.

The conventional silicon-cell array is about 9 percent efficient in space. By contrast, the efficiency of the proposed dispersion system that uses an optimistically efficient optical system and a solar-cell array using hypothetical (and similarly optimistically efficient) solar cells is projected at no more than 8 percent.

Lewis Research Center,
National Aeronautics and Space Administration,
Cleveland, Ohio, April 4, 1967,
120-33-01-10-22.

APPENDIX - SYMBOLS

A	constant, dependent on material
B	constant, dependent on material
B_{ij}	area proportional to solar intensity in $\Delta\lambda_{Hj}$ in $\Delta\theta_4$ band
B_j	area proportional to total solar intensity in $\Delta\lambda_{Hj}$
C	constant, dependent on material
E_r	total refracted energy at refracting surface
f	focal length
$H(\lambda)$	solar spectral intensity
H_{λ_j}	total solar intensity in wavelength range $\Delta\lambda_{Hj}$, $\text{mW}/(\text{cm}^2)(0.02 \mu\text{m})$
K	constant
N	spectral refractive index of vacuum, assumed to be 1
n_λ	spectral refractive index
P_i	output power per unit area from each group of spectral cells
$R(\lambda)$	equal energy relative response
r_p	light reflected parallel to plane of incidence at refracting surface
r_s	light reflected perpendicular to plane of incidence at refracting surface
x	distance from focus to prism-reflector plane (fraction of focal length)
y	distance from optic axis to any point on prism-reflector plane
α	plus or minus 16' of arc
β	prism wedge angle, deg
δ	deviation angle between cone ray and normal ray, both striking prism reflector at same point, deg
η	total array energy-conversion efficiency
η_i	efficiency of standard 10-percent silicon solar cell when illuminated by light of range $\Delta\lambda'_{1,2}$
η_{si}	efficiency of typical 10-percent silicon cell
θ_1	incidence angle of white light on prism reflector first surface, deg
$\theta_{1,2}$	angle of refracted beam at first surface of prism reflector, deg

θ_2	incidence and reflection angles at reflecting surface of prism reflector, deg
θ_3	incidence angle of refracted ray at prism-reflector third surface (inside prism reflector), deg
θ_4	angle at which rays emerge from prism reflector, deg
$\Delta\theta_4$	total dispersion of spectrum from prism reflector
$\theta_{4,a}, \theta_{4,b}$	angle of ray emerging from prism reflector and striking solar-cell array at limits of any spectral band defined by λ_a and λ_b
λ	any specific wavelength
λ_1, λ_2	equal response points wavelengths on silicon spectral-response curve
λ_1^+, λ_2^+	positive and negative cone wavelengths defined at $(\theta_{4,a} - \theta_{4,b})/2$, or array $1/2^0$ point
λ_a, λ_b	wavelength defined by any $\Delta\theta_4$
$\Delta\lambda$	wavelength interval
$\Delta\lambda_{1,2}^+$	wavelength interval from dispersed beam
$\Delta\lambda_{Hj}$	increment of solar-intensity wavelength, $0.02 \mu\text{m}$
φ	angle between negative cone ray and optic axis
φ'	angle between normal ray (1) and optic axis at focus
φ_1	incidence angle at any refracting surface
φ_2	refraction angle at any refracting surface
Subscripts:	
a, b	limits of array area occupied by particular type of solar cell
B	blue light, $0.36 \mu\text{m}$
i	incremental distance on solar array
j	wavelength increment of $0.02 \mu\text{m}$
R	red light, $1.2 \mu\text{m}$
+	positive
-	negative
λ	light of any wavelength

REFERENCES

1. Klucher, Thomas M.: Theoretical Performance of Solar Cell Space Power Systems Using Spectral Dispersion. II - Dispersion by Diffraction Grating. NASA TN D-4157, 1967.
2. Jenkins, Francis A.; and White, Harvey E.: Fundamentals of Physical Optics. McGraw-Hill Book Co., Inc., 1937, p. 289.
3. Hodgman, Charles D., ed.: Handbook of Chemistry and Physics. 39th ed., Chemical Rubber Co., Cleveland, 1957, p. 2728.
4. Jenkins, Francis A.; and White, Harvey E.: op. cit., p. 390.
5. Jenkins, Francis A.; and White, Harvey E.: op. cit., p. 398, figure 18L.

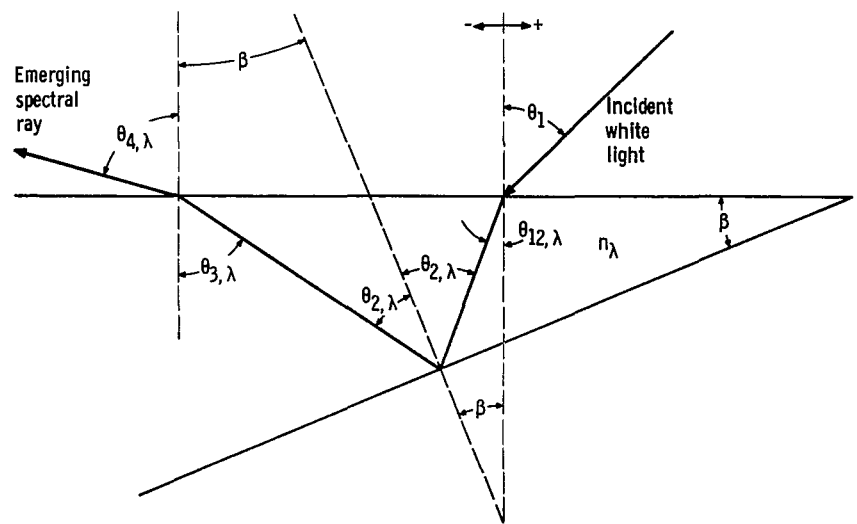
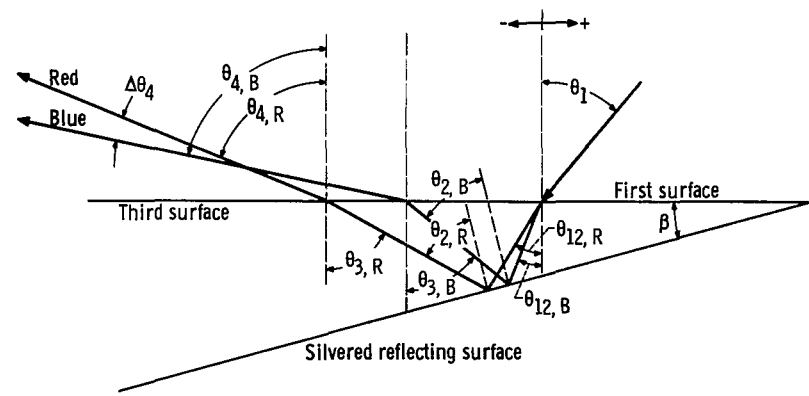
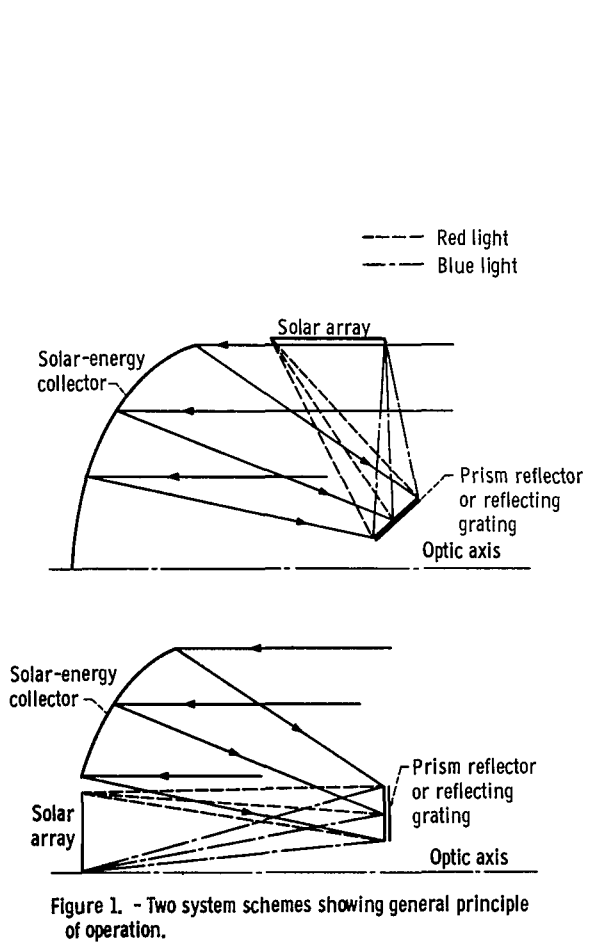


Figure 2. - Prism reflector.

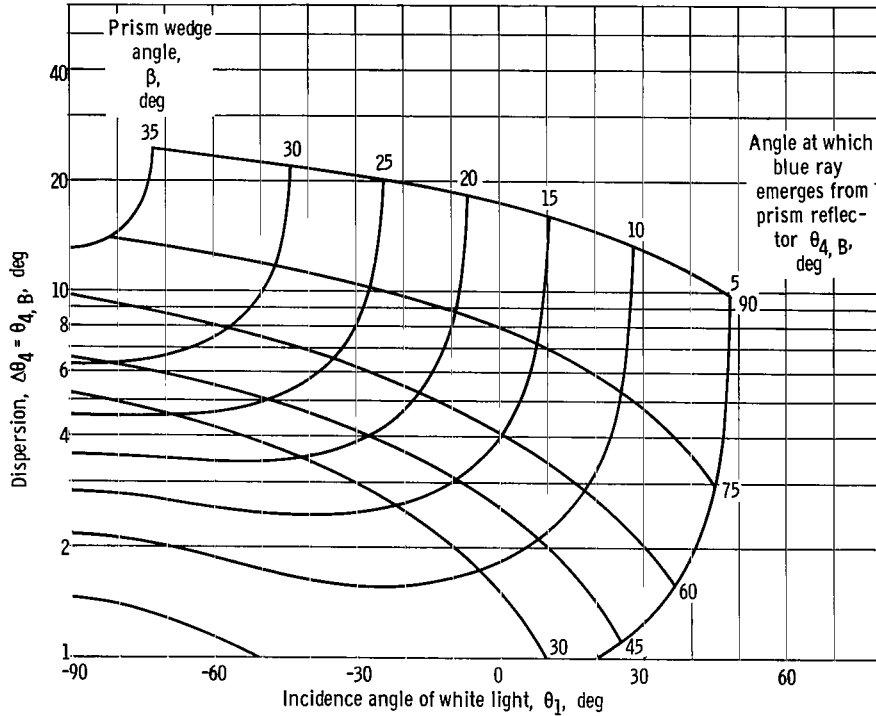


Figure 3. - Variation of emerging blue beam as function of prism parameters. Specific wavelength, 0.36 microns.

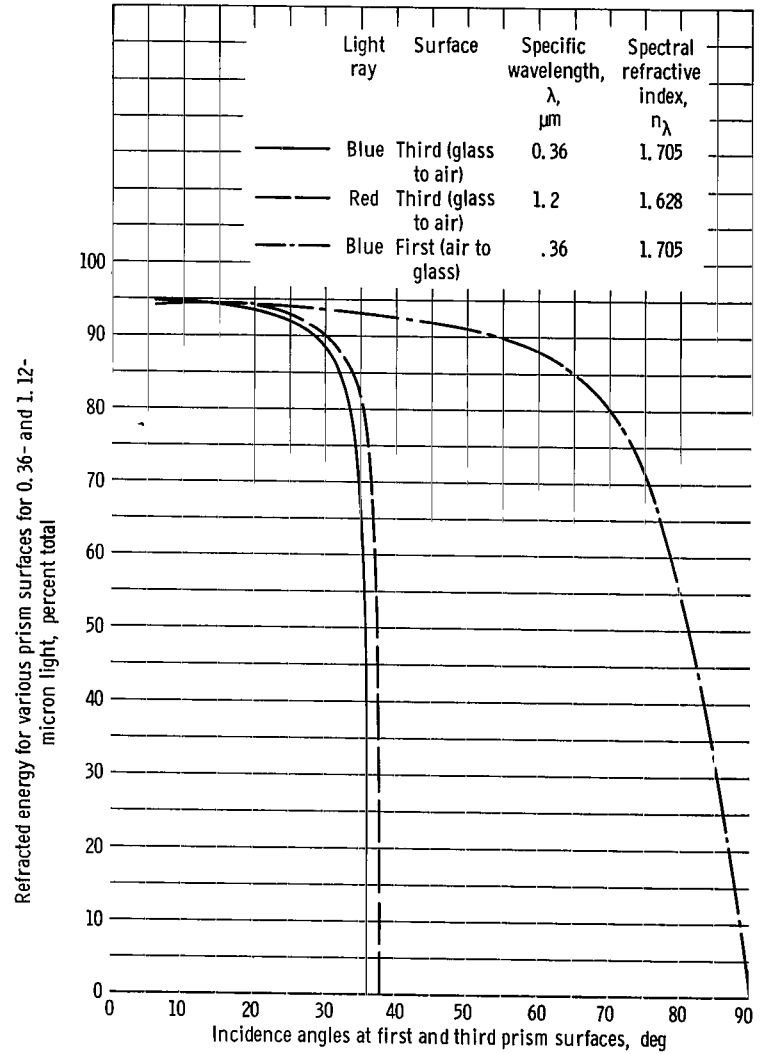


Figure 4. - First and third prism-surface spectral transmission for blue light ($\lambda = 0.36 \mu\text{m}$) and red light ($\lambda = 1.2 \mu\text{m}$).

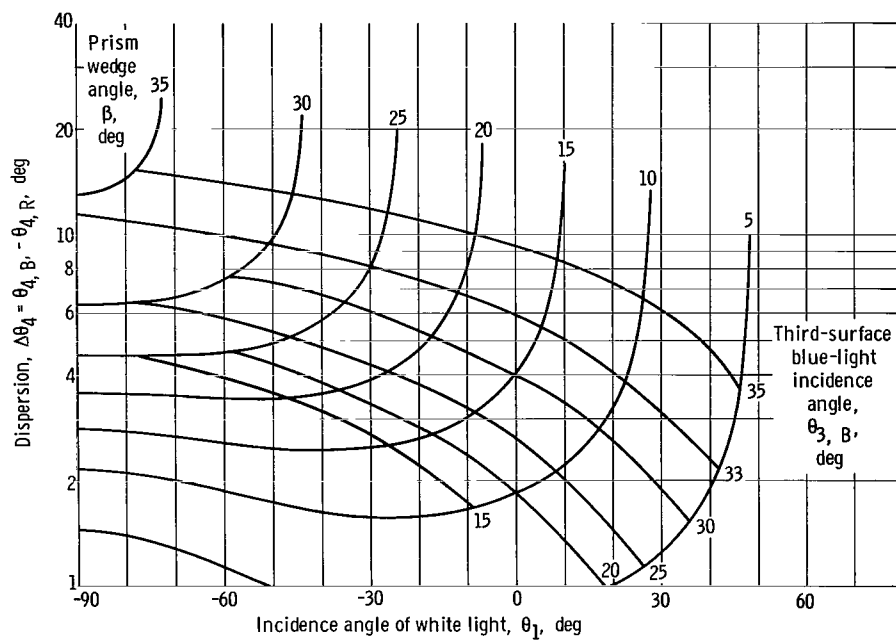
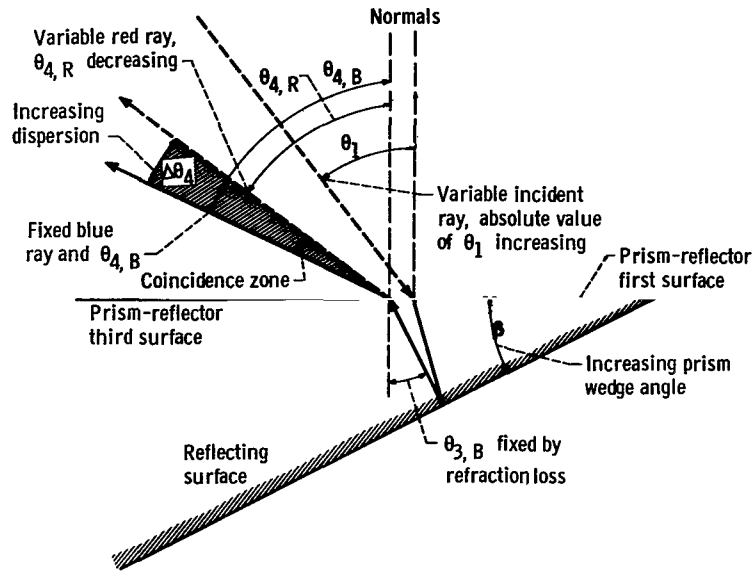
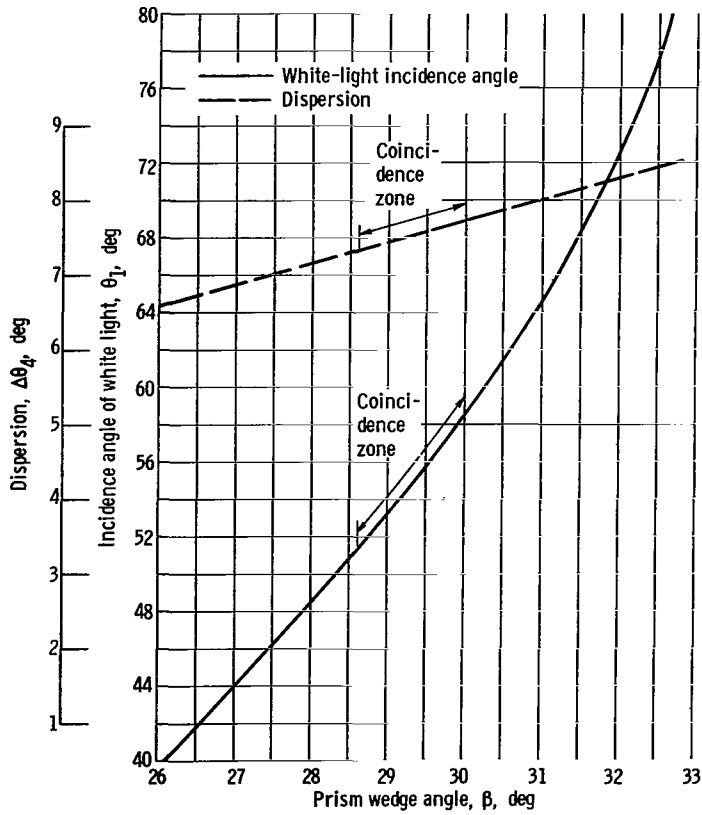


Figure 5. - Third-surface blue-light incidence angle as function of prism parameters. Specific wavelength, 0.36 micron.



(a) Diagram of effect.



(b) Effect.

Figure 6. - Effect of system restraints on dispersion.

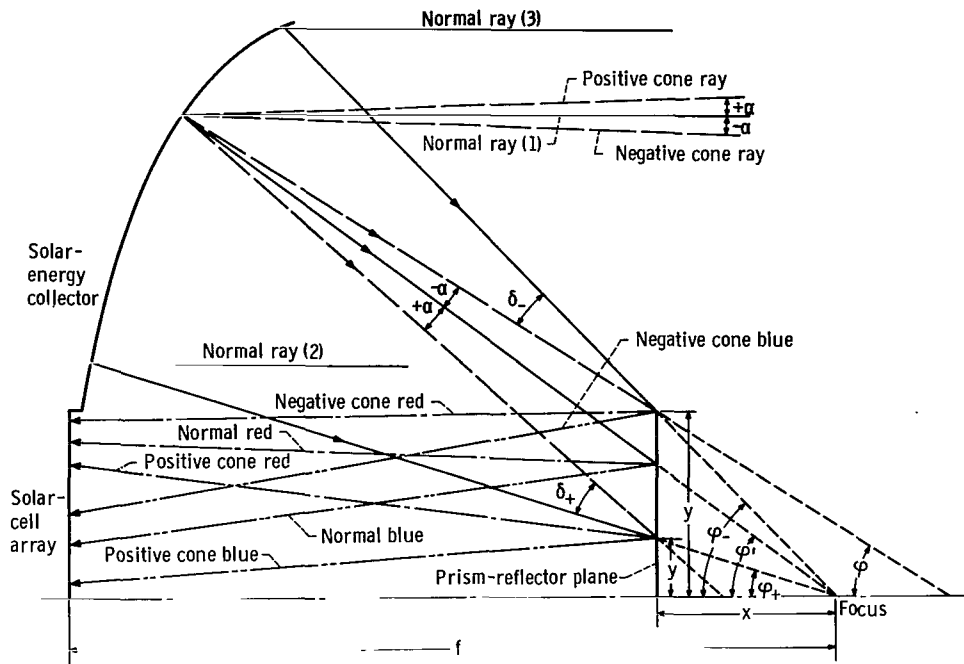


Figure 7. - One-dimensional effect of cone of light at prism plane.

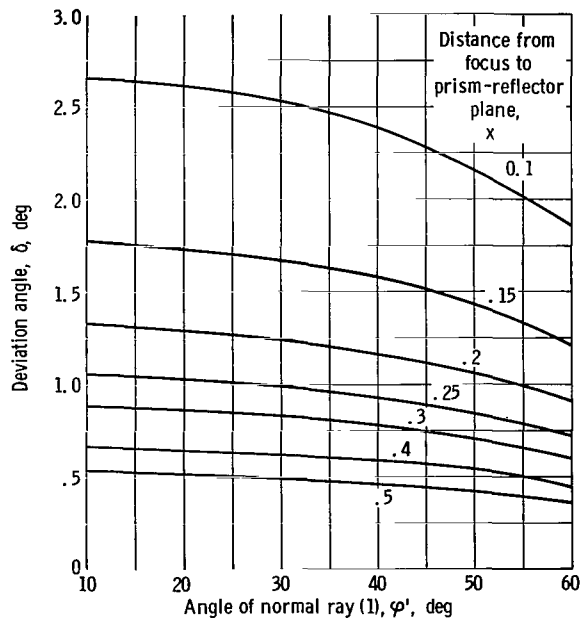


Figure 8. - Deviation angle of positive cone ray and normal ray as function of prism position on mirror optic axis.

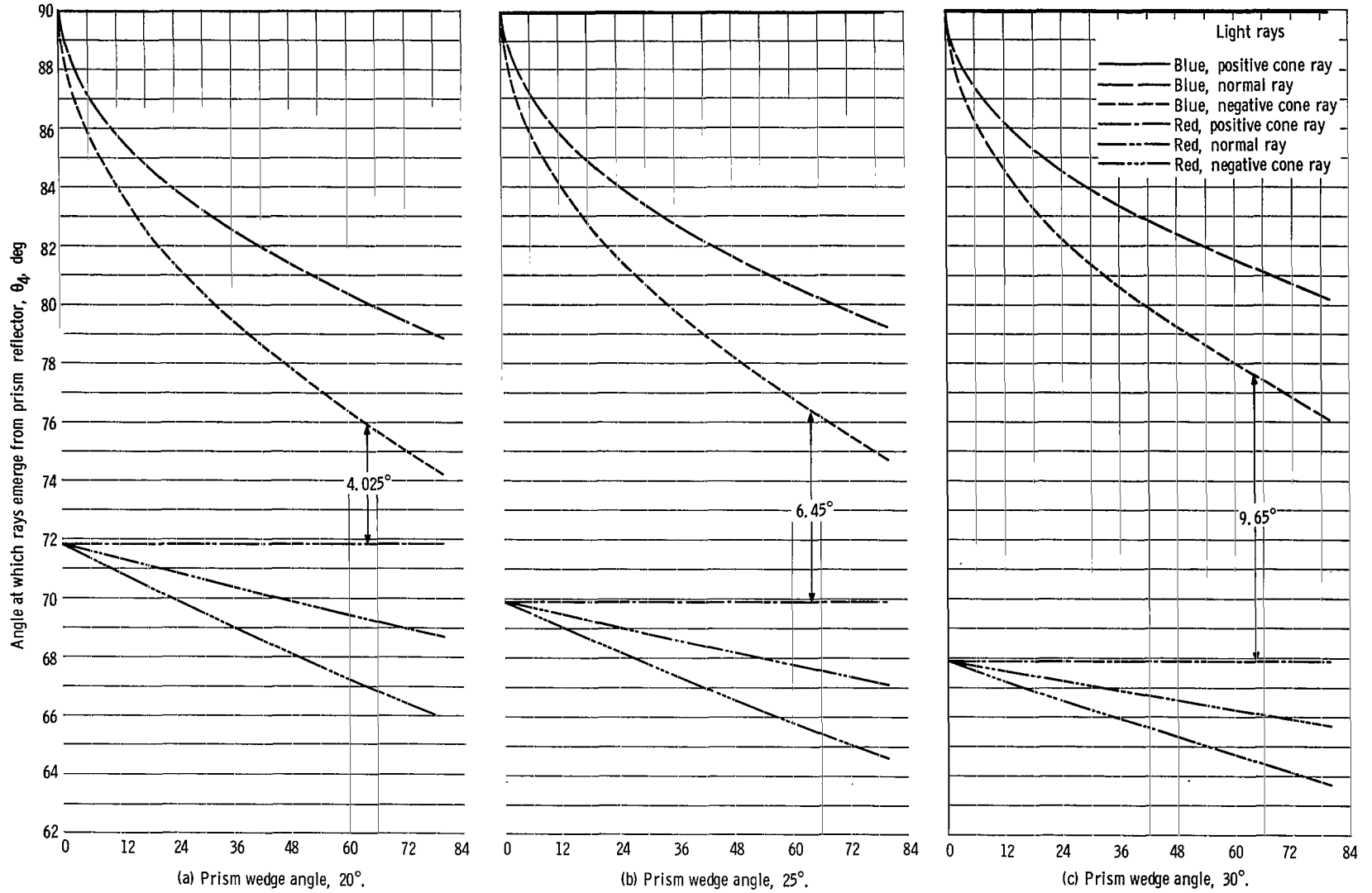


Figure 9. - Defocusing of 0.36- and 1.2-micron beams due to cone of light. Spectral refractive index of vacuum, 1; blue ray, 1.705; red ray, 1.628.

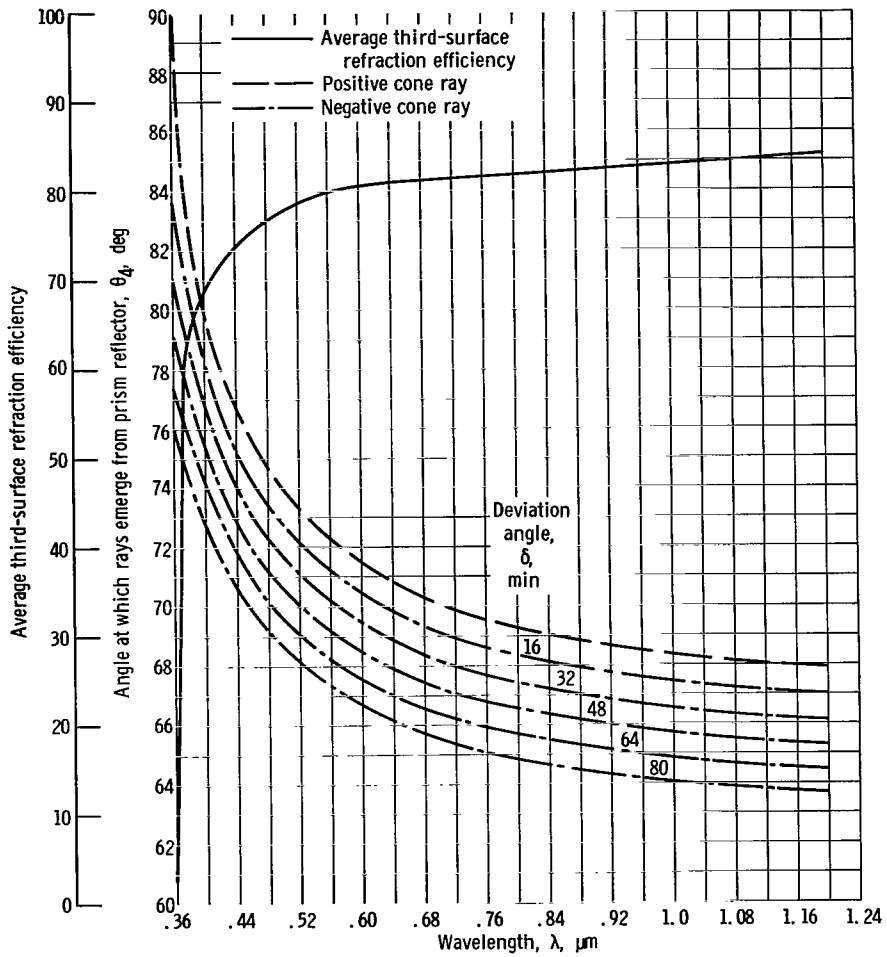


Figure 10. - Spectral quality of dispersion beam with partial cone-of-light effects. Prism wedge angle, 30° ; spectral refractive index of vacuum, 1; blue ray, 1.705; red ray, 1.628.

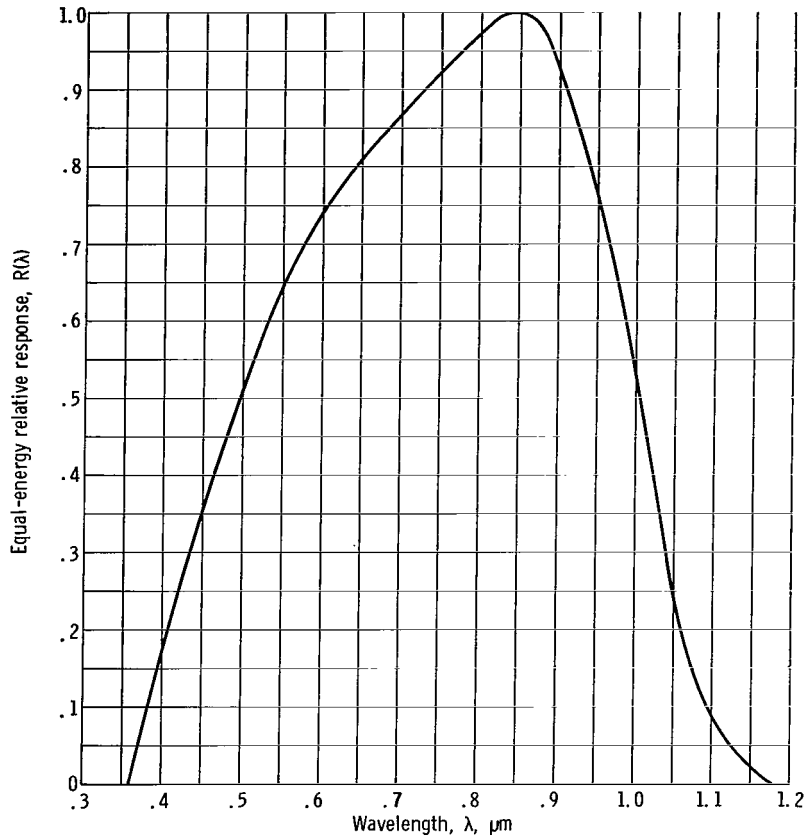


Figure 11. - Spectral response of n-p silicon cell.

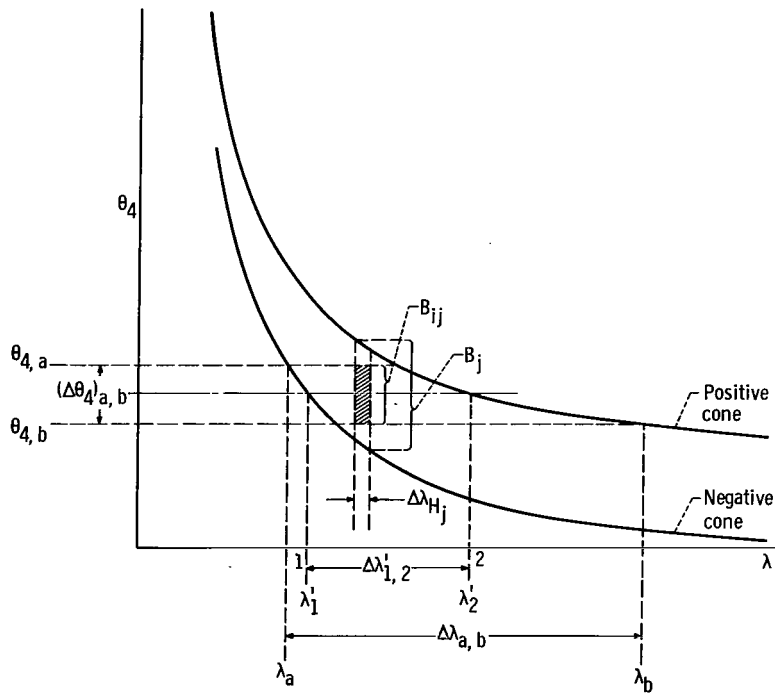


Figure 12. - Description of weighted solar-intensity calculation.

"The aeronautical and space activities of the United States shall be conducted so as to contribute . . . to the expansion of human knowledge of phenomena in the atmosphere and space. The Administration shall provide for the widest practicable and appropriate dissemination of information concerning its activities and the results thereof."

—NATIONAL AERONAUTICS AND SPACE ACT OF 1958

NASA SCIENTIFIC AND TECHNICAL PUBLICATIONS

TECHNICAL REPORTS: Scientific and technical information considered important, complete, and a lasting contribution to existing knowledge.

TECHNICAL NOTES: Information less broad in scope but nevertheless of importance as a contribution to existing knowledge.

TECHNICAL MEMORANDUMS: Information receiving limited distribution because of preliminary data, security classification, or other reasons.

CONTRACTOR REPORTS: Scientific and technical information generated under a NASA contract or grant and considered an important contribution to existing knowledge.

TECHNICAL TRANSLATIONS: Information published in a foreign language considered to merit NASA distribution in English.

SPECIAL PUBLICATIONS: Information derived from or of value to NASA activities. Publications include conference proceedings, monographs, data compilations, handbooks, sourcebooks, and special bibliographies.

TECHNOLOGY UTILIZATION PUBLICATIONS: Information on technology used by NASA that may be of particular interest in commercial and other non-aerospace applications. Publications include Tech Briefs, Technology Utilization Reports and Notes, and Technology Surveys.

Details on the availability of these publications may be obtained from:

SCIENTIFIC AND TECHNICAL INFORMATION DIVISION
NATIONAL AERONAUTICS AND SPACE ADMINISTRATION

Washington, D.C. 20546